Chapter 1

Introduction

1.1 ETH Polyproject *Variability of the Sun and Earth's Climate*

This thesis is carried out within the ETH-Polyproject *Variability of the Sun and Earth's Climate*. The project's main aim is to study to what extent the solar irradiance variations - besides the man-made influences - have an effect on the Earth's climate. To answer this question it is in the first place essential to gain a solid understanding of the origins of the total and spectral irradiance variations. The main assumption is that the solar surface magnetic field is responsible for the variations. This assumption is first verified on the variability of the total solar irradiance (TSI), which then allows to go one step further and apply it for the description of the spectral solar irradiance (SSI) variability. This allows the reconstruction of the SSI for times when no observations are available. Having solar irradiance data available for a time scale of two decades, the coupling with the Earth's climate can be studied in detail. As the projects aim yields at an understanding of the Sun and the Earth's climate system - two separate research fields - the best platform is an inter-disciplinary project, like the present Polyproject, consisting of four subprojects which are shortly outlined in the following.

Subproject I aims at the physical origins of the solar irradiance variability. In particular, the assumption that the solar irradiance variability can be fully described by changes of the surface magnetic field has been verified and applied to reconstruct the total solar irradiance (TSI) on the basis of the analysis of space-based and ground-based magnetograms of the solar disk (Wenzler et al., 2004; Wenzler et al., 2005; Wenzler et al., 2005a).

Subproject II, the main focus of the present thesis, aims at the reconstruction of the solar UV variability. The motivation for this work is that the solar UV varies by up to a factor of 2 over the solar cycle time scale. Rozanov et al. (2002) have shown that the spectral variability of the UV has a wavelength dependent effect on the ozone and temperature in the stratosphere. Thus, it is important to understand the physical origins of the solar UV variability. Here we take the same approach as in Subproject I and apply their analysis of space-based and ground-based magnetograms for the reconstruction of the UV.

Then, in Subproject III the coupling of the solar variability to the Earth's atmosphere is studied. The effect of variations of the solar irradiance, in particular the spectral variability with an emphasis on the UV radiation, ozone and other trace gases, is studied in detail. Further, their influence on the dynamics and temperature of the atmosphere, from the mesopause down to the Earth's surface is studied on the basis of steady-state simulations.

Finally, in Subproject IV the climate system response to the solar variability is studied with transient ensemble experiments. An improved understanding of the Sun-Earth coupling

mechanisms - in particular a coupling due to the varying UV radiation - is the main goal the project. As the Sun is the main research object of the thesis a brief introduction to its evolution, the structure of the solar atmosphere, the origin of the emergent radiation, is given in the following.

1.2 The Sun

1.2.1 Evolution

The evolution of a star strongly depends on its mass. In the following the evolution of a star with one solar mass is briefly outlined.

When an interstellar cloud collapses due to the gravitional force being stronger than the internal gas pressure, the density and temperature in its center increase such that hydrogen fusion is ignited. This is considered as the birth of a star. A long and stable phase is associated with the fusion of hydrogen into helium, the hydrogen *burning*, hydrogen in the core being used up and transformed into helium. During this phase the star belongs to the main sequence in the Hertzsprung-Russel diagram. When most of the core hydrogen is exhausted, the hydrogen burning continues in the layers around the core, and the star leaves the main sequence. By expanding and brightening, it will become a red giant. Successively, the hydrogen burning shell is moving towards outer layers. This leads to the situation where pressure and gravity are not in equilibrium anymore and the star collapses, increasing the temperature and density in the core again to such a degree that helium burning is activated. In the following, when helium is used up in the core, the helium fusion goes on in an steadily outward moving shell.

At a certain point the hydrogen burning shell reaches layers where the temperature and density decrease, and follwoingly the hydrogen fusion ceases. Due to the radiation pressure the remaining hydrogen envelope is pushed off, whereby a planetary nebulae is created. Also the helium burning shell ends when it reaches the outer layers of the star. Then the final state of a star with one solar mass, a white dwarf, is reached. According to Schaller et al. (1992) a zero age main sequence (ZAMS) star with one solar mass has a luminosity of $0.687\,L_\odot$ ($L_\odot$ being the (present) solar luminosity), whereas, when the hydrogen burning ceases, 9.96 Gyr after zero age, its luminosity is $1.66\,L_\odot$. The increase in luminosity will have considerable consequences for the conditions on Earth, e.g. the terrestrial climate.

At present time our Sun is in the quasi-steady state of a main sequence star. Its energy output is, however, not constant in an absolute sense, but varying on different time scales and energy scales. Its variation covers the particle flux of the solar wind as well as the electromagnetic spectrum, the latter, in particular the UV, being of main interest for the present work.

1.2.2 Solar atmosphere

The varying electromagnetic spectrum, from X-ray to radio flux, emerges from different heights in the solar atmosphere. Thus, the structure of the solar atmosphere is of great importance for the understanding of the variability of the solar spectrum. Its vertical stratification can be described according to its change of temperature with height.

The innermost layer of the solar atmosphere is the photosphere where the temperature decreases with height and which emits radiation at visible wavelengths. Then, the temperature minimum of about $T = 3600$ to 4 900 K, depending on the region (Fontenla et al., 1999, 2005),

is the layer of the solar atmosphere where the temperature no longer decreases but begins to increase with height. The core of photospheric absorption lines is formed close to the temperature minimum. Next, in the chromosphere the temperature increases to up to 10^5 K. Hydrogen starts to become partially ionized. The UV and extreme ultra-violet (EUV), e.g. Lyman α and the cores of Ca II H and K, are formed in this layer. The transition region, showing a very steep temperature increase, separates the chromosphere from the corona, the latter forming the most outward layer, having temperatures larger than 10^6 K and where the atoms are highly ionized (Avrett & Murdin, 2000).

1.2.3 Variability of the solar irradiance

The solar irradiance varies over a wide range of time scales and amplitudes. The main reason for these changes is that the Sun oscillates in a wide range of modes from minutes to years (Fröhlich & Lean, 2004). Associated with these changes are a series of observed inhomogeneous features on the Sun, which amongst others are the granular cell and network pattern for the quiet Sun, and active regions of varying brightness like bright network, faculae and plage, as well as sunspots, and flares associated with an active Sun. A fundamental question is: Can the luminosity changes be described by other observables associated with solar activity?

In fact, in recent years a number of observables have been found to be correlated with the changes of the solar irradiance, which are the Mg II index (Heath & Schlesinger, 1986; Fröhlich, 2002), Ca II K flux (Ermolli et al., 2003), the 10.7 cm radio flux (Tapping, 1987), He I λ 10830 equivalent width, the Be^{10} flux in the Earth's atmosphere (Beer et al., 1990), the aa geomagnetic index (Cliver et al., 1998), the open magnetic flux (Solanki et al., 2000) or a combination of proxies (Fligge & Solanki, 1998). Also a change in the solar diameter has been proposed to be correlated with solar irradiance variations (Thuillier et al., 2005).

Yet, the longest record of solar activity goes along with the sunspot number, which has been regularly observed since the invention of the telescope in 1608 (Eddy, 1976). The definition of the sunspot number is $R = k(f + 10g)$, where g is the number of visible sunspot groups, f is the total number of individual spots (Murdin, 2000). The scaling factor k is applied to correct for differences due to observational sights, observers and instrumental effects (Hoyt & Schatten, 1998). It has been shown that the sunspot number tracks the 11-year solar cycle (Schwabe, 1844) of the TSI very well (Aldrich & Hoover, 1954; Fröhlich & Lean, 2004). Yet, as the effective temperature of sunspots is lower than of the quiet Sun, sunspots alone can not describe the increase in radiation at solar maximum. It is the bright features associated with the sunspots that compensate for the dimming of the sunspots and lead to an increase in radiation. Both, sunspots and faculae are caused by the solar surface magnetic field, being flux tubes of different size (Solanki, 2003). Sunspots have a lower effective temperature due to suppressed convection, whereas it is the hotter walls of small flux-tubes (Spruit, 1976), which cause the faculae appear brighter, in particular they reveal a higher contrast on the limb than at disk center, as at disk center the hot wall of a vertical flux tube is out of line-of-sight. Spruit (2000) claim that reduced cooling in spots and enhanced emission by small scale magnetic fields are the most effective mechanisms and account for most of the observed variations.

Sunspots and faculae - as well as network and plage - have their origin in the solar surface magnetic field (Stenflo, 1994; Solanki, 1999, 2003; Ortiz et al., 2000). Therefore, it is consequent to use the magnetic field to describe solar irradiance variations. Following Wenzler et al. (2005); Wenzler et al. (2005a); Krivova et al. (2003), we describe the solar variability by changes of the magnetic field strength on the solar surface.

1.3 Previous work in TSI and SSI reconstruction

1.3.1 Correlative Studies

There have been a number of attempts to reconstruct the spectral solar irradiance (SSI) and total solar irradiance (TSI) by directly relating solar activity indices with irradiance. Fligge et al. (1998) apply the changing distribution of the magnetic features of the solar surface to describe irradiance variations over two solar cycles. Fligge & Solanki (2000) extended this approach and included a slowly varying solar surface magnetic network into the reconstruction. Lean (2000) use a wavelength-dependent parameterization of the spectral irradiance variability derived from contemporary measurements and extend it back in time applying historical estimates for facular brightening and sunspot darkening. Further, the correlative model *Solar2000* by Tobiska (2004) relates irradiance at a particular wavelength to that of other wavelengths and solar indices. Krivova & Solanki (2005) use solar UV observations to extrapolate synthetic spectra to shorter wavelengths and then reconstruct the UV on the basis of magnetograms. Correlative studies aim to produce optimal TSI and SSI reconstructions, but lack a physical explanation of the processes responsible for the solar variability. To gain a better physical understanding of the processes, we aim at reconstructing the SSI employing a physics based spectral synthesis code together with the solar surface magnetic field as index.

1.3.2 Physics-based models

A different approach from directly relating solar activity indices is an approach applied by several authors to calculate intensity spectra with a radiative transfer code. Then the intensity spectra are weighted according to the distribution of active regions derived by the detailed analysis of various solar images.

First, the Spectral And Total Irradiance Reconstruction (SATIRE) models (Unruh et al., 1999; Fligge et al., 2000a,b; Fligge & et al., 2000; Krivova et al., 2003) employ the assumption that the irradiance changes are entirely due to changes of the solar surface magnetic field. They base the calculation of intensity spectra, carried out by Unruh et al. (1999), on the plane-parallel ATLAS9 code by Kurucz (1991). This code allows the calculation of spectra in local thermodynamic equilibrium (LTE). With a 4-component model, accounting for the contribution of umbra, penumbra, sunspots and faculae, they reconstruct the TSI, as well as the SSI for the three filter channels of VIRGO (Variability of solar IRradiance and Gravity Oscillations,Fröhlich et al. (1995); Fröhlich et al. (1997) and Fröhlich & Lean (2004)). For the UV this approach is not appropriate, as below 2000 Å it is essential to employ non-LTE radiative transport calculations (Haberreiter et al., 2002).

Ermolli et al. (2003), Penza et al. (2004) calculate synthetic spectra with the LTE radiative transfer code SPECTRUM (Gray & Corbally, 1994) and derive the distribution of active regions from the Ca II K and continuum flux images taken with the Precision Solar Photometric Telescope (PSPT, Coulter et al. (1996)), at the Rome observatory and at the Mauna Loa Solar Observatory on Hawaii. Fox et al. (2004) calculate synthetic spectra with the plane-parallel non-LTE radiative transfer code SunRISE and reconstruct the solar variability on the basis of PSPT images. Recently, Fontenla et al. (2005) presented the improved Solar Radiation Physical Modeling (SRPM), a continuation of the SunRISE model.

As the time series of continuous observations of the solar magnetic field started much earlier than the beginning of the PSPT observation, we apply the analysis of the solar magnetic field measurements by Krivova et al. (2003); Wenzler et al. (2005a) as a proxy for the SSI

variability. The difference to their approach is that we employ the non-LTE radiative transfer code COSI (cf. Chapter 4) to calculate solar intensity spectra for the quiet Sun, sunspots and plage. This allows to include the rising temperature profile of the chromosphere, essential for the calculation of synthetic spectra. As the solar atmosphere structures are an important input for the spectrum synthesis, a brief overview of is given in the following section.

1.3.3 Empirical atmosphere structures

The main input for calculating synthetic spectra are the atmosphere structures representing the quiet Sun and different active regions an the solar disk. Assuming little interaction between the various types of features, it is a first approximation to construct separate one-dimensional models that describe the vertical structure of the horizontally distinct regions.

Kurucz (1991) gives a grid of atmosphere structures for different gravitational accelerations and effective temperatures, which allow to choose the suitable atmosphere structure for the quiet Sun and active regions according to their effective temperature. These model atmospheres give temperature and column density as a function of height for the photosphere up to the temperature minimum. Krivova & Solanki (2005); Wenzler et al. (2004); Wenzler et al. (2005); Wenzler et al. (2005a,b) employ the atmosphere structures for $\log g = 4.44$ and effective temperatures $T_{\text{eff}} = 4500$ K and T_{eff} =5400 K for umbrae and penumbrae respectively for the reconstruction of the TSI.

Fontenla et al. (1999, 2005) developed model atmospheres structures corresponding to the quiet Sun (referred to as FAL-C) and active regions, e.g. the plage model, FAL-P, and the sunspot model, FAL-S. The structures are derived by adjusting the temperature as a function of height, including the chromosphere, for each brightness component so that the calculated spectrum agrees as well as possible with observations. The corresponding density distribution is determined from a balance between gas and turbulent pressure and solar surface gravity. Krivova & Solanki (2005); Wenzler et al. (2004); Wenzler et al. (2005); Wenzler et al. (2005a,b) use modified versions of FAL-C and FAL-P for the quiet Sun and faculae (cf. Unruh et al., 1999), further referred to as U99-C and U99-P, which in their version do not include the rising temperature profile of the chromosphere, and the temperature gradient of the plage model has been slightly changed.

1.4 Structure of the thesis

The aim of the present thesis is the reconstruction of the solar irradiance with an emphasis on the UV part of the solar spectrum. To achieve this aim, we precede as follows.

In Chapter 2 the UV measurements taken by the Solar Ultraviolet Spectral Irradiance Monitor (SUSIM) and Solar/Stellar Irradiance Comparison Experiment (SOLSTICE) onboard the Upper Atmosphere Research Satellite (UARS) are discussed. For the time when observations are available, they serve as valuable means to verify the reconstructions. Therefore, it is important to study the uncertainty of the observations before they are applied for validation.

Next, in Chapter 3, a brief introduction to the radiative transfer in general and an overview of the structure of COSI is given.

In Chapter 4 the radiative transport code COSI is discussed in detail. In its original setup the code was not applied for solar studies. Thus, certain implementations had to be carried out in order to achieve a realistic spectrum synthesis. The most important implementations are (1) the solar atmosphere structures, (2) the explicit non-LTE atomic levels, (3) the photo-

ionization cross sections, (4) the improvement of the cross sections of negative hydrogen and (5) the non-LTE opacity distribution functions (ODFs). The effect of different abundances and atmosphere structures on the LTE and non-LTE calculation is discussed in detail. Also, the change of the populations numbers with the iterations of the ODFs is investigated.

Next, in Chapter 5 the line spectra calculated with COSI are presented and compared to other synthetic spectra and available observations.

Then, in Chapter 6 we present first reconstructions based on the available analysis of magnetograms by Krivova et al. (2003), Wenzler et al. (2004); Wenzler et al. (2005); Wenzler et al. (2005a), going back to 1974.

In Chapter 7 we carry out a sensitivity study to analyze the contribution of the different active regions to the UV variability. Furthermore, the latest reconstructions, based on spectrum synthesis, including all the implementations discussed, are presented.

Chapter 2

Observed solar spectra

2.1 Introduction

Observations of solar spectra are the basis to study its variability. As the Earth's atmosphere absorbs wavelengths shorter than ~ 3000 Å, it is imperative to measure the solar UV radiation from space. In Table 2.1 an overview of the different instruments, measuring the UV at various wavelengths, temporal and spectral resolution is given. Measurements of the Lyman α (H I λ 1216) from space started in 1947 (Woods et al., 1998, 2000), being followed by the EUVS experiment on the Atmospheric Explorer E (AE-E) (Hinteregger et al., 1981), the UV spectrometer on the Solar Mesospheric Explorer (SME) (Rottman, 1981) and later by the Upper Atmosphere Research Satellite (UARS) in late 1991. The Thermosphere Ionosphere Mesosphere Energetics and Dynamics (TIMED) spacecraft has started January 2002, since when the Solar Extreme Ultraviolet Experiment (SEE) takes daily, full-disk measurements to up to 2000 Å. With the SOlar Radiation and Climate Experiment (SORCE) being launched early 2003, additional time series of UV observations became available with the Solar Stellar Irradiance Comparison Experiment (SOLSTICE) and the Spectral Irradiance Monitor (SIM).

The SOLSPEC measurements onboard of three ATLAS missions, undertaken in March 1992, April 1992, and November 1994, measured the solar spectrum from 2000 Å to 8700 Å, with a resolution of 10 Å below Lyman α, 2.5 Å from Lyman α to 4000 Å, and 5 Å above 4000 Å. NSO/Kitt Peak FTS measurements (Wallace et al., 1998) give ground based high resolution spectra for disk center.

As we are interested in the long-term variability of the solar spectral irradiance, e.g. disk integrated flux, in the wavelength range from 1000 to 4000 Å, we focus in the following on the measurements taken by the Solar Ultraviolet Spectral Irradiance Monitor (SUSIM) and Solar/Stellar Irradiance Comparison Experiment (SOLSTICE) onboard the UARS. Not only do these instruments observe at the wavelength range under investigation, they also record the longest time series of UV measurements from space.

Recently, Thuillier et al. (2004) published a composite for two solar activity levels, ranging from 5 to 24 000 Å. That, together with the UARS measurements serve as a valuable means to validate the UV synthetic spectra and reconstructions. In the following the data is discussed in more detail. First, SUSIM comprises daily, 10 Å gridded irradiances (version 21, level 3BS) for the wavelengths from 1155 to 4105 Å and for the time span from September 11, 1991 to April 27, 2002 (available at ftp://susim.nrl.navy.mil/pub/uars/). A newer version will be available by the end of 2005. The SOLSTICE instruments gives spectral irradiances for the wavelength range from 1195 to 4195 Å, for 10 Å-bins on a daily basis. Version 18 (available at ftp://disc1.gsfc.nasa.gov/data/uars/solstice/) includes the time span from September

Instrument	Carrier	Period		Wavelength	Resolution		Mode
		Begin	End	(Å)	sp. (Å)	temp.	
various	rockets	1947	pres.	1216	var.	-	irr
EUVS	AE-E	1977	1980	140-1850	2-54	0.5 s	irr
UV spectr.	SME	1981	1989	1150-3030	10	-	irr
SUSIM	UARS	09/11/1991	pres.	1155-4105	10	1 day	irr
SOLSTICE	UARS	09/11/1991	pres.	1195-4195	10	1 day	irr
SOLSPEC	ATLAS 1	03/1992	-	2000-8700	>2.5	-	irr
SOLSPEC	ATLAS 2	04/1993	-	2000-8700	>2.5	-	irr
SOLSPEC	ATLAS 3	11/1994	-	2000-8700	>2.5	-	irr
SEE	TIMED	07/12/2001	pres.	< 2000	10	3 min	irr
SIM	SOURCE	25/01/2003	pres.	3100-20000	1-340	1 day	irr
SOLSTICE	SOURCE	25/01/2003	pres.	1150-3100	10	1 day	irr
NSO/KP FTS	ground			3570 - 7405	0.0076	-	rad

Table 2.1: Instruments measuring the solar spectrum for different spectral, temporal and spatial resolution. The Mode *irr* stands for measuring the disk integrated flux normalized to 1 AU, whereas *rad* stands for the measurement at a certain position on the solar disk.

11, 1991 to September 23, 2000. In the upper panel of Fig. 2.1 the irradiances for the 10 Å-bin centered at 1215 Å, including Lyman α (1216 Å), measured by SUSIM (dotted line) and SOLSTICE (dashed line) are compared. They change up to a factor of 2 over the solar cycle. Before mid 1994 both data sets agree well, however after that time they show a considerable discrepancy. Also, the SUSIM data show a stronger and more extended decrease towards the minimum. Additionally, early 1996, the SUSIM data show a sudden decrease, not present in the SOLSTICE data, which increases the discrepancy between both data sets. This comparison indicates the uncertainties present in spectral irradiance measurements.

2.2 Observations

In Fig. 2.1 the spectra taken with both instruments on March 25, 1997 are compared. On the logarithmic scale both spectra do not show considerable deviations, only below 1300 Å the SUSIM data show lower values. To study the uncertainty of the different spectral bins of both instruments we compare the maximal and minimal values of the whole time series of both data sets. Here we use a 7-day mean not to account for the short-term variability. Fig. 2.2 shows the ratio of the spectral irradiance measured by the SUSIM instrument (S_{SUSIM}) to the SOLSPEC instrument (S_{SOLSPEC}) for the minimum values (dotted line) and the maximum values (solid line). Below 1400 Å both ratios show similar values, indicating an offset between both instruments. Furthermore, there are wavelengths where the measurements by the SUSIM instrument are up to 20 % higher, and others where they are up to 10 % lower. Below 1400 Å the minimum value of the SUSIM instrument is generally higher than the SOLSTICE measurement, whereas it is the reverse for the maximum values. This indicates that in this wavelength range the SUSIM instrument exhibits a higher variability than the SOLSTICE instrument. To further study this effect, the relative spectral variabilities measured by both instruments are compared in Fig 2.3. The SUSIM instrument shows a higher variability below 1400 Å, whereas above 1400 Å both instruments measure a comparable spectral variability. Yet, from 2000 to 3000 Å the SUSIM variability is slightly lower. These considerations demonstrate

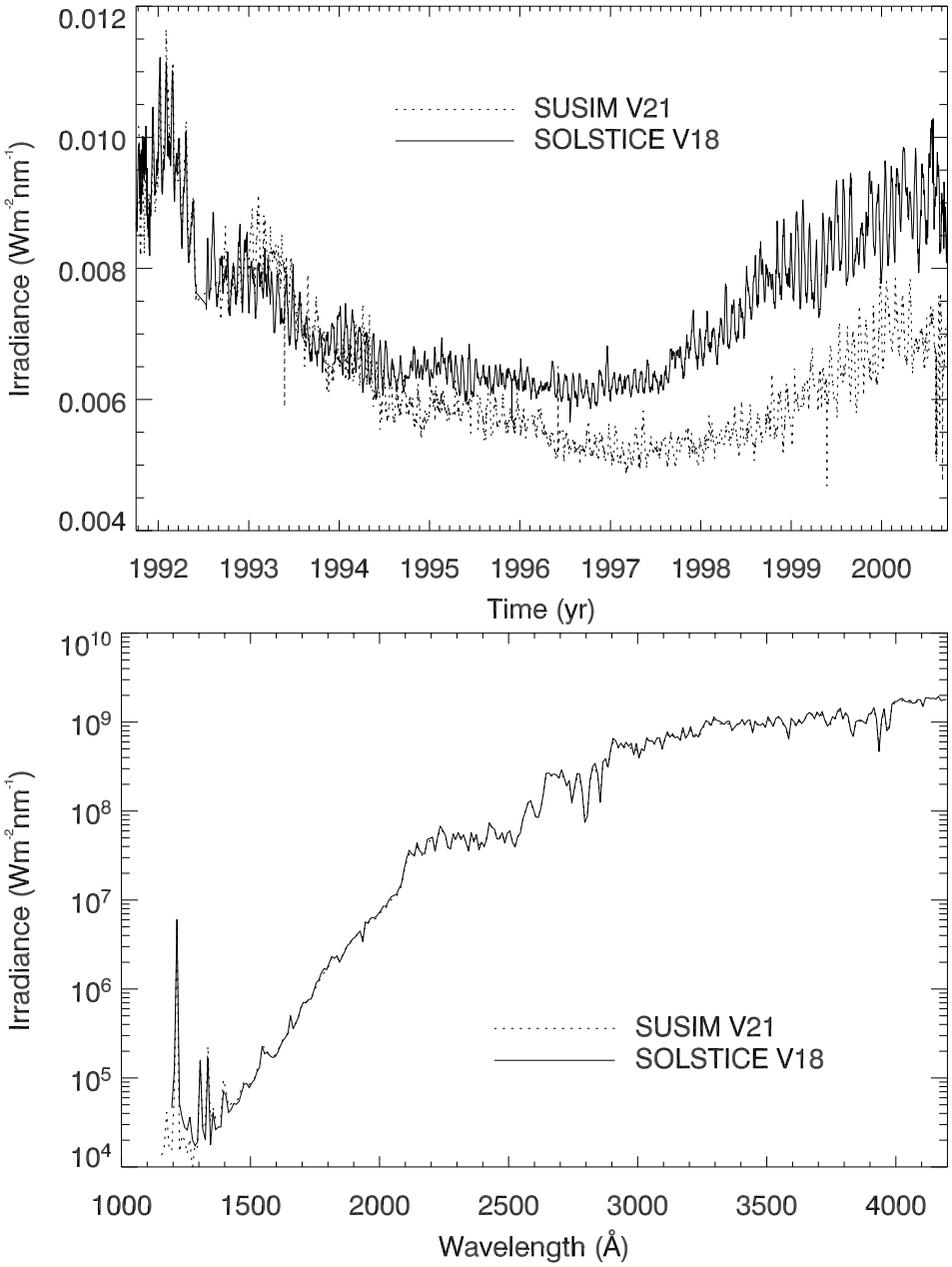

Fig. 2.1: The upper panel shows the comparison of the temporal variation of the SUSIM data (dotted line) and SOLSTICE data (solid line) for the 10 Å-bin centered at 1215 Å containing Ly α. The irradiance at that wavelength increases by a factor of ~ 2 over the solar cycle. On the lower panel the comparison of SUSIM and SOLSTICE spectra - taken on 3/25/1997. Generally, both spectra agree well, only below 1300 Å do the SUSIM data show a lower irradiance.

that the observations of the spectral solar irradiance show substantially absolute and relative uncertainties.

Another interesting question is how well the spectral irradiance bins in the UV correlate with other wavelengths. To answer this question the correlation coefficients between the irradiance of each spectral bin and the irradiance at 1215 Å is shown in Fig. 7.3 for the SUSIM instrument (dotted line) and the SOLSTICE instrument (dashed line). The SOLSTICE observations show an overall correlation coefficient of > 0.6, except at 2100 Å. Thus, according the SOLSTICE data the variability of the UV generally follows the Lyman α variability well.